Characterising mean and extreme diurnal variability of ocean CO2 system variables across marine environments

Olivier Torres, Lester Kwiatkowski, Adrienne J. Sutton, Narimane Dorey, James C Orr

Characterising mean and extreme diurnal variability of ocean CO$_2$ system variables across marine environments

Olivier Torres[1], Lester Kwiatkowski[2], Adrienne J. Sutton[3], Narimane Dorey[1], James C. Orr[4]

[1]Laboratoire de Météorologie Dynamique, IPSL/ENS, Ecole Normale Supérieur 24 rue Lhomond, Paris, France
[2]LOCEAN Laboratory, Sorbonne Université-CNRS-IRD-MNHN, Paris, 75005, France
[3]NOAA Pacific Marine Environmental Laboratory, Seattle, United States of America.
[4]Laboratoire des Sciences du Climat et de l'Environnement, LSCE/IPSL, CEA-CNRS-UVSQ, Université Paris-Saclay, Ormes des Merisiers, Bât 714, F-91191 Gif-sur-Yvette, France.

Corresponding author: Olivier Torres (olivier.torres@lmd.ens.fr)

Key Points:

- Multi-year 3-hourly observations of CO$_2$ system variables are used to assess diurnal and seasonal variability across marine environments.

- Amplitudes of extreme diurnal variations in pCO$_2$, pH, and Ω_{arag} are often comparable to those of seasonal cycles.

- The balance between different drivers of diurnal and seasonal CO$_2$ system variability differs across timescales and environments.

Abstract

Diurnal variability of ocean CO_2 system variables is poorly constrained. Here this variability and its drivers are assessed using 3-hourly observations collected over 8-140 months at 37 stations located in diverse marine environments. Extreme diurnal variability, i.e. when the daily amplitude exceeds the 99th percentile of diurnal variability, is comparable in magnitude to the seasonal amplitude and can surpass projected changes in mean states of pCO$_2$ and $[H^+]$ over the twenty-first century. At coastal sites and near coral reefs, extremes in diurnal amplitudes reach 187±85 and 149±106 μatm for pCO$_2$, 0.21±0.08 and 0.11±0.07 for pH, and 1.2±0.5 and 0.8±0.4 for Ω_{arag}, respectively. Extreme diurnal variability is weaker in the open ocean, but still reaches 47±18 μatm for pCO$_2$, 0.04±0.01 for pH, and 0.25±0.11 for Ω_{arag}. Diurnal variability of the ocean CO_2 system is considerable and likely to respond to increasing CO_2. Therefore, it should be represented in Earth system models.

Plain language summary

Our understanding of how ocean pH and related chemical variables vary during the day (known as diurnal variability) is not well established. Here we use a recent dataset of such observations collected every 3 hours during 8 to 140 months from 37 buoys located across the oceans to assess these diurnal variations and what drives them. In extreme cases, observed changes over 24 hours were found to be greater than those observed between seasons. Diurnal variations in these chemical variables are particularly large in coastal waters and near coral reefs and are not negligible further offshore. Along with the more gradual, long-term acidification of the ocean from atmospheric CO_2 increases year after year, diurnal and seasonal variability of ocean chemistry is also expected to change dramatically. Understanding how this diurnal variability will change in the future is important because it modulates the levels of acidification experienced by marine organisms from long-term yearly changes.

1- Introduction

1.1 Climatic change and ocean acidification

The human and environmental impact of climate change is a consequence of changes in both mean climate and low probability, high intensity climatic extreme events. Observations over land indicate broad evidence of increasing heat waves (Pachauri et al., 2014) and intensifying maximum daily precipitation (O'Gorman, 2015). Extremes in both precipitation (Palmer & Räisänen, 2002) and temperature (Meehl & Tebaldi, 2004) are projected to increase throughout the twenty-first century. In the ocean, assessment of extremes has focused on marine heat waves, their increased frequency during the last 30 years, and their projected dramatic increase during this century (Frölicher et al., 2018; Hobday et al., 2016). In contrast, extremes in ocean CO_2 system variables on similarly short timescales are only beginning to be assessed (Burger et al., 2020) although changes in their mean states and seasonal variations are well understood. Here to bridge the time gap, we have assessed observed diurnal variability of ocean CO_2 system variables, comparing its drivers to those of seasonal variability. This assessment offers a first step to provide a benchmark for the long-term goal of including diurnal variability of ocean CO_2 system variables in Earth system models, as needed to make projections of ocean acidification more relevant to critical timescales that affect marine organisms.

Rising concentrations of CO_2 in the atmosphere result in gradual ocean acidification (Caldeira & Wickett, 2003; Orr et al., 2005) leading to a lower capacity for seawater to buffer changes in CO_2 system variables (Feely et al., 2004; Gattuso & Hansson, 2011). The global average pH of the open ocean is estimated to have decreased by 0.018 units per decade over 1991-2011 (Lauvset et al., 2015), with open-ocean time series stations showing declines of 0.017 to 0.027 units per decade in the last 15-30 years (Bates et al., 2014; Bindoff et al., 2019). Earth system models (ESM) project that by the end of the 21st century, the global-mean

pH will decrease by 0.16 to 0.44 (low and high-emissions scenarios SSP1-2.6 and SSP5-8.5, respectively), relative to 1870-1899 values (Kwiatkowski et al., 2020). These changes and related changes in other CO_2 system variables may adversely affect marine organisms. For instance, it is thought that protein synthesis (Langenbuch et al., 2006), olfactory discrimination (Munday et al., 2009), and predator-prey responses (Watson et al., 2017) may be sensitive to increases in pCO_2 and hydrogen ion concentration $[H^+]$ in fish and marine invertebrates although some of these sensitivities have been recently questioned (Clark et al., 2020). Organisms that construct shells and skeletons of calcium carbonate ($CaCO_3$) may be particularly sensitive (Kroeker et al., 2010). Chemical conditions relevant to calcification have been expressed in terms of the calcium carbonate saturation state (Ω). This coefficient is specific to the calcite or aragonite calcium carbonate polymorph formed: $\Omega_{arag/calc} = [Ca^{2+}][CO_3^{2-}]/K_{sp}$, where K_{sp} is the apparent solubility product of calcite or aragonite, and the numerator is the product of the in situ calcium and carbonate ion concentrations. The formation of $CaCO_3$ is favored at higher Ω values, with many studies showing that declines in species-specific and ecosystem-level calcification are correlated with decreasing Ω_{arag} (Albright et al., 2016, 2018; Chan & Connolly, 2013; Kroeker et al., 2010).

1.2 Acidification variability and extremes

Natural variability of ocean CO_2 system variables is partly driven by biological processes, such as photosynthesis-respiration and $CaCO_3$ calcification-dissolution (Schulz & Riebesell, 2013). In the coastal ocean in particular, CO_2 system variables are influenced by seasonal processes such as changes in temperature, seasonal upwelling of CO_2-rich waters, freshwater discharge, and biological activity (e.g. Hauri et al., 2009; Salisbury et al., 2008; Thomsen et al., 2010). The combination of these biological and physical drivers can result in large seasonal changes in carbonate chemistry. For instance in a 1-year study in the Aegean Sea,

where blooms are limited by oligotrophic conditions, winter and summer pCO_2 differed by up to 208 µatm (González-Dávila et al., 2016). Autonomous surface buoys deployed over 8-140 months have also detected seasonal pCO_2 amplitudes (winter-summer differences) of up to 330 µatm in coastal environments and up to 70 µatm in the open ocean (Shadwick et al., 2015; Sutton et al., 2019). Coastal sites monitored over several years reveal differences of up to 1.2 pH units within a single month, with the most extreme values of pH exhibiting large interannual variability (e.g. Dorey et al., 2013; Pecquet, Dorey and Chan, 2017).

While seasonal and interannual variations are relatively well characterized, diurnal variations in CO_2 system variables are less so because they require high-frequency measurements. However it is known that diurnal pCO_2 variability is thermally driven in the open-ocean Sargasso Sea, with typical diurnal amplitudes of 5-25 µatm and an extreme amplitude of 50 µatm observed during a hurricane (Bates et al., 1998). Furthermore, higher diurnal amplitudes for pCO_2 (100-500 µatm) and pH (0.2-0.5 units) have been recorded near benthic ecosystems such as coral reefs, (Drupp et al., 2013; Koweek et al., 2015; Shamberger et al., 2011), kelp forests (Murie & Bourdeau, 2020), and seagrasses (Berg et al., 2019), particularly in shallow waters, where the ratio between benthic biomass and overlying seawater volume is enhanced (Hofmann et al., 2011; Page et al., 2019).

1.3 Changing seawater chemistry variability

Observations show that, on average, the amplitude of the seasonal cycle of surface ocean pCO_2 has increased by about 2 µatm per decade from 1982 to 2015 (Landschützer et al., 2018). With a continued increase, ESMs project a 1.5 to 3-fold average amplification of the seasonal amplitude of pCO_2 over the twenty-first century under the RCP8.5 high-end emissions scenario (Gallego et al. 2018; McNeil and Sasse 2016). Similar amplification is projected for the seasonal amplitude of the hydrogen ion concentration $[H^+]$ but not for that of

pH (-16%), the change in which represents a proportional change in $[H^+]$ seasonal amplitude relative to the annual mean state of $[H+]$, the latter which increases even faster than the former (Kwiatkowski et al., 2020; Kwiatkowski & Orr, 2018). There is also a projected decline in the seasonal amplitude of surface ocean Ω_{arag} (-9%). These different responses result from varying sensitivities of these variables to atmospheric CO_2 (Hagens & Middelburg, 2016a) and from climate change, which drives diverging trends in the seasonal extremes of the principal controlling variables (temperature, DIC, and A_T; Kwiatkowski & Orr, 2018). Diurnal variability of ocean CO_2 system variables also appears to be greatly affected by increasing atmospheric CO_2, as suggested by data from shallow CO_2 vents (Kerrison et al., 2011), where background pCO_2 levels approach those expected for the global average late in the twenty-first century under the RCP8.5 scenario (Kwiatkowski & Orr, 2018). Hence there is need to characterize these diurnal variations across the ocean and assess how they will be affected by ocean carbon uptake and climate change.

Changes in the seasonality of ocean CO_2 system variables may modify the response of marine organisms to ocean acidification. Seasonal variations affect the timing of thresholds such as when Ω transitions from supersaturated to undersaturated conditions (Gruber et al., 2012; McNeil & Matear, 2008; Sasse et al., 2015). They also affect the intensity of biological impacts, with recent perturbation studies indicating that chemical variability on hourly timescales may increase the metabolic costs of acidification in molluscs (Mangan et al., 2017) and echinoderms (Small et al., 2016). Given that hourly variability of ocean CO_2 system variables can have ecosystem-level implications (e.g. affect coral reef calcification rates; Albright et al., 2016, 2018), characterising the magnitude of diurnal CO_2 system variability and how it might change in the future may be critical to projecting the biological impacts of ocean acidification.

Here we use a new collection of 3-hourly observations from 37 stations across multiple ocean basins (Sutton et al., 2019) to assess the diurnal variability of surface ocean pCO$_2$, pH, [H$^+$], and Ω_{arag}. We evaluate the processes that control this variability across different ecosystem types, comparing extremes in diurnal variability to mean diurnal and seasonal variability.

2 – Methods and Data

2.1 Data

The *in situ* observational database used here is that from Sutton et al. (2019). We assess data from 37 fixed station time series across four ocean basins (26 in the Pacific, 9 in the Atlantic, 1 in the Indian, and 1 in the Southern Ocean). These stations are spread among three types of ecosystems (16 in the open ocean, 11 in the coastal ocean, and 10 near coral reefs) as indicated in Figure 1. Station bottom depths are >1000 m for open-ocean stations, 16-780 m for coastal stations, and 3-23 m for coral reef stations (Table S2).

For each station, we used observations of sea surface temperature (T), salinity (S), CO$_2$ partial pressure (pCO$_2$), and where available, pH. The observational methodology is fully described by Sutton et al., (2014). In brief, T and S were collected at approximately 0.5 m using a Sea-Bird Electronics 16plus V2 SeaCAT or a SBE 37 MicroCAT sensor. The pH measurements were made with either a spectrophotometric Sunburst SAMI-pH sensor (Seidel et al., 2008) or an ion sensitive field effect transistor (SeaFET) pH sensor (Bresnahan et al., 2014; Martz et al., 2010), with an associated uncertainty of < 0.02 pH units. The mole fraction of CO$_2$ (xCO$_2$) is measured at ~0.5 m with an automated equilibrator□based gas collection system and an infrared gas analyzer (LI□820, LI□COR™). Seawater pCO$_2$ is then calculated with respect to standard operating procedures (Dickson et al., 2007; Weiss, 1974), with

uncertainty of < 2 µatm (Sutton et al., 2014). The combined set of time series span from 2004 to 2017 although the duration at any station varies between 8 and 140 months.

2.2 Reconstruction of pH data and carbonate chemistry calculations

Despite extensive pCO$_2$ observations, simultaneous pH measurements across the stations were limited, with only 18 stations providing more than 100 pH measurements (Table S1). Thus we reconstructed pH at all 37 stations from pCO$_2$, A_T, S, and T. A_T was reconstructed from T and S, using region-specific empirical relationships from Lee et al., (2006). This approach was chosen for its computational efficiency and general applicability. Comparison of results to those made with the same approach but with a regionally specific algorithm (Xue et al., 2016) were found to have limited impact on the resulting pH (e.g., a root mean square difference of 0.01 pH units between the two algorithms at Gray's Reef station). We then calculated pH and Ω_{arag} from A_T and measured pCO$_2$, T, and S (available at all 37 stations) using *CO2SYS-MATLAB* (van Heuven et al., 2011) and the constants recommended for best practices (Dickson et al., 2007; Orr et al., 2015). For input, these calculations also included total dissolved inorganic phosphorus and total dissolved silicon concentrations taken from the nearest grid cell of the annual-mean World Ocean Atlas climatology (Garcia et al., 2013).

Reconstructed pH was compared to in situ pH measurements at the 18 stations that had sufficient data with a focus on mean values and diurnal and seasonal variability (Table S1, Figures S6-S7). There is generally good agreement between the reconstructed and measured diurnal cycles of pH and [H$^+$] across stations (Figure S7), an indication that the reconstructed AT was not strongly influenced by localized biology that is uncorrelated with physical changes. The average root mean square error (RMSE) between observed and reconstructed pH was 0.024 (Table S1), while the largest RMSE values were at the Stratus (0.0656) and Iceland (0.0558) stations. The multi-station mean correlation between observed and

reconstructed pH is $r^2 = 0.82$, while 15 out of 18 stations have an $r^2 > 0.6$ (Table S1). Thus, the pH calculated from measured $p\text{CO}_2$ and reconstructed A_T appears adequate for this assessment of diurnal and seasonal variability. This finding is in agreement with previous studies that have assessed the same station data for seasonal variability (e.g. Sutton et al., 2016) and can be attributed to several factors: 1) At all stations, use of the $p\text{CO}_2$-A_T pair means that propagated uncertainties for calculated pH, [H$^+$], and Ω_arag are dominated by uncertainties in $p\text{CO}_2$ with uncertainties in A_T having relatively little effect (Orr et al., 2018); 2) At the coral reef stations, the impact of net ecosystem calcification on surface ocean A_T is typically small with measured values similar to those of nearby open-ocean waters (Drupp et al., 2013); and 3) At stations where benthic ecosystem calcification does influence surface ocean A_T (e.g. CRIMP2), the magnitude of calcification-driven variability is much smaller than that of net ecosystem production (Drupp et al., 2013; Shamberger et al., 2011).

In contrast, large diurnal variability in A_T has been reported at some coral reef sites (e.g. Koweek et al., 2015), which if due to localized biology and uncorrelated with physical changes would mean that the corresponding reconstructed pH is a poor estimator of true pH. However, such disagreement was not detected in our analysis of the Sutton et al. (2019) dataset.

2.3 Diurnal, extreme diurnal and seasonal variability

Across all stations, diurnal and seasonal variability of CO_2 system variables were assessed, with a particular focus on extreme diurnal variability. To standardize observed variations to similar day-night conditions, the Coordinated Universal Time recorded at each station was converted to local time. All but one of the stations were confined to the low and mid-latitudes (Table S2). To compute the diurnal cycle at each station, days were excluded if any of the 3-hourly observations were missing. Thus between 106 and 2688 complete diurnal cycles were obtained at the different stations (Table S2). Within each diurnal cycle at each station, the

diurnal peak-to-peak amplitude (daily maximum – minimum) was computed for pCO$_2$, pH, [H$^+$], and Ω_{arag}. The distribution of the computed diurnal amplitudes was subsequently used to calculate days with extreme diurnal variability, here defined as days where that amplitude is above the 99th percentile. The diurnal variability on those extreme days at a given station is taken as its extreme diurnal variability. The total number of days having extreme diurnal variability ranged from 1 to 26 among stations due to differences in the length of their observational records. Our approach to characterize extreme diurnal variability probabilistically at the local scale is consistent with the general approach used to characterize temperature extremes (e.g. Frölicher et al., 2018). However the extreme diurnal variability will differ relatively more between stations in our case because CO$_2$ system variability is strongly influenced not only by ocean circulation and mixing but also by the productivity of local ecosystems, a factor that varies greatly between the open and coastal ocean, particularly near coral reefs (Drupp et al., 2013; Koweek et al., 2015; Yan et al., 2011), kelp forests (Murie & Bourdeau, 2020), and seagrasses (Berg et al., 2019).

To compute seasonal variability, stations were included in our analysis if their time series contained at least two complete diurnal cycles for each month of the calendar year. Thus, seasonal cycles were obtained from 23 out of the 37 stations, with seasonal amplitudes calculated from monthly mean values as the peak-to-peak amplitude in a calendar year. Thirteen of those stations had more than one complete seasonal cycle, which were used to construct monthly climatologies (Table S2).

2.4 Decomposing drivers of variability

The effects of temperature (T), salinity (S), dissolved inorganic carbon (DIC), and total alkalinity (A_T) in driving diurnal, extreme diurnal and seasonal cycles of pCO$_2$ across the three ecosystem types were assessed using a Taylor-series deconvolution (Takahashi et al., 1993):

$$\Delta pCO_2 \approx \left(\frac{\partial pCO_2}{\partial DIC}\right)\Delta DIC + \left(\frac{\partial pCO_2}{\partial A_T}\right)\Delta A_T + \left(\frac{\partial pCO_2}{\partial T}\right)\Delta T + \left(\frac{\partial pCO_2}{\partial S}\right)\Delta S \qquad (1)$$

where all Δ terms are diurnal or monthly anomalies (relative to the daily or annual mean), and the partial differentials (sensitivities) are estimated numerically using the *CO2SYS-MATLAB derivnum* routine (Orr et al., 2015). Given that A_T is estimated from T and S, its variability reflects changes in water masses and assumes no influence of localized biology when that is uncorrelated with physical changes. Uncertainties in A_T will also affect DIC, which is computed from the pCO_2-A_T input pair. The deconvolution was made independently for each diurnal and seasonal cycle before averaging across multiple cycles at each station. For the diurnal analysis, the results from those deconvolutions were then further averaged across each station type.

3 - Results

3.1 Diurnal and extreme diurnal carbonate chemistry variability

At open-ocean stations, the mean diurnal amplitudes were 9±4 μatm for pCO_2, 0.008±0.003 for pH, 0.17±0.07 nmol kg^{-1} for [H$^+$], 0.05±0.02 for Ω_{arag}, and 0.06±0.05 for S (on the practical salinity scale), all provided as the multi-station mean ± inter-station standard deviation (Figure 2). This limited mean diurnal variability was associated with low coincident variations in T (0.35±0.14°C) and was similar across all open-ocean stations located in the Atlantic, Pacific, and Indian Oceans. Conversely, the corresponding extreme diurnal variability was greater. When averaged over the days having extreme diurnal variability, the mean diurnal amplitudes at open-ocean stations were 47±18 μatm for pCO_2 0.04±0.01 for pH, 0.89±0.33 nmol kg^{-1} for [H$^+$], 0.25±0.11 for Ω_{arag}, 0.54±0.46 for S and 1.82±1.10°C for T (Figure 2). The amplitudes of these extremes in diurnal variability were comparable to the

amplitudes of the average seasonal cycles of pCO_2 (49±23 µatm), pH (0.05±0.03), [H^+] (0.94±0.49 nmol kg^{-1}), and S (0.54±0.26). On the other hand, extreme diurnal amplitudes of T and Ω_{arag} in the open-ocean are smaller than the corresponding seasonal amplitudes (5.03±2.7°C and 0.43±0.17, respectively).

Mean diurnal variability of these CO_2 system variables was consistently higher at coastal stations than in the open ocean (Figure 2). Across coastal stations, the amplitude of mean diurnal variability was 36±16 µatm for pCO_2, 0.04±0.02 for pH, 0.71±0.31 nmol kg^{-1} for [H^+], 0.21±0.10 for Ω_{arag}, 0.59±0.49 for S, and 0.73±0.17°C for T. This variability, although considerable, is enhanced greatly during days with extreme diurnal variability, reaching amplitudes of 178±82 µatm for pCO_2, 0.21±0.08 for pH, 3.54±1.54 nmol kg^{-1} for [H^+], 1.11±0.48 for Ω_{arag}, 4.65±2.82 for S, and 3.0±0.66°C for T. These extreme diurnal amplitudes are comparable to the seasonal amplitudes of pCO_2 (210±76 µatm), pH (0.23±0.08), [H^+] (4.19±1.60 nmol kg^{-1}), and Ω_{arag} (1.17±0.37). The extreme diurnal amplitude for T is lower than the corresponding seasonal amplitude (8.12±4.04 °C), while for S it is greater than the seasonal amplitude (2.32±1.68).

Observations from coral reefs also exhibit enhanced diurnal variability in CO_2 system variables relative to the open ocean, with mean diurnal amplitudes of 50±49 µatm for pCO_2, 0.04±0.04 for pH, 0.90±0.89 nmol kg^{-1} for [H^+], 0.28±0.24 for Ω_{arag} (Figure 2). Also enhanced relative to the open ocean are the diurnal amplitudes of the physical drivers: 0.20±0.16 for S and 0.55±0.24 °C for T. Still further enhanced are the amplitudes of extreme diurnal variability: 149±106 µatm for pCO_2, 0.11±0.07 for pH, 2.71±1.91 nmol kg^{-1} for [H^+], 0.80±0.40 for Ω_{arag}, 2.63±2.82 for S, and 1.7±0.6°C for T. As already seen for coastal observations, the amplitudes during days with extreme diurnal variability at coral-reef sites were comparable to those for the observed seasonal cycles of pCO_2 (90±56 µatm), pH (0.08±0.05), and Ω_{arag} (0.40±0.50), but lower than the seasonal amplitude of T (3.9±2.0 °C)

and higher than the seasonal amplitude of S (1.16±0.64) and [H^+] (1.74±1.04 nmol kg^{-1}). The high inter-station standard deviation for the variability of CO_2 system variables at coral reef stations when compared to that at coastal stations comes from one coral-reef station in the Pacific (CRIMP2), which exhibited particularly high variations. Across the other coral-reef stations, the inter-quartile range of diurnal and extreme diurnal variability of CO_2 system variables was generally lower than across coastal stations (Figure 2).

3.2 Contrasting diurnal and seasonal drivers of pCO$_2$

Despite nonlinearities in the CO_2 system, the deconvolution generally provides a reasonably accurate reconstruction of the observed pCO$_2$ anomalies across timescales and ecosystem types (Figure 3). Across all stations and temporal scales, the effect of salinity on diurnal and seasonal cycles of pCO$_2$ is negligible (Figure 3).

At open-ocean stations, mean diurnal cycles of pCO$_2$ are dominated by changes in T and moderated somewhat by changes in DIC (Figure 3a). For the extreme diurnal variability, the DIC-driven changes become as important as the thermal component and are responsible for the mid-day maximum (Figure 3d). For seasonal variations in pCO$_2$, the thermal component once again dominates at open-ocean stations, except at equatorial stations where seasonal variations are weak (Figures 3, S1). Typically, temperature-driven seasonal pCO$_2$ anomalies are only partially compensated by opposing changes in DIC, a pattern that is well established for the low latitudes, where most of our stations are located (Sarmiento & Gruber, 2019; Takahashi et al., 1993, 2014).

Across coastal and coral reef stations, mean diurnal and extreme diurnal variability of pCO$_2$ is driven by variations in DIC and attenuated slightly by coincident and opposing thermally driven changes (Figure 3, b,c,e,f). At coastal stations, diurnal changes in A_T enhance this thermal attenuation but remain quite small. Seasonal variability of pCO$_2$ at

coastal stations is also generally dominated by variations in DIC and moderated by variations in temperature and A_T (Figure 3) except at Grays reef where thermally driven variations dominate (Figure S2). Yet at coral reef stations, seasonal variability of pCO_2 is dominated by themal variations (Figures 3, S3).

4 – Discussion and conclusions

4.1 Processes influencing diurnal variability

Changes in surface DIC can be driven by net primary production and air-sea gas exchange or by physical processes, such as through lateral advection or vertical exchange with DIC-rich deep water via upwelling or mixed layer entrainment and detrainment. The diurnal cycles of DIC that drive diurnal variability in pCO_2 at the coastal and coral reef stations exhibit maxima around 06:00 and minima during 15:00-18:00 (Figure 3). These peaks are likely the result of net respiration throughout the night followed by light dependent increases in net primary production, with similar cycles widely documented on coral reefs (Drupp et al., 2013; Page et al., 2019; Shamberger et al., 2011) and in other productive coastal environments (e.g. Berg et al., 2019; Hofmann et al., 2011; Murie & Bourdeau, 2020). Advection and gas exchange would not be expected to influence diurnal DIC anomalies in the same manner and are thus presumed to be second-order effects.

Open ocean stations exhibit pCO_2 maxima at noon, when waters are warmest, highlighting the different controls on diurnal cycles compared to coral reef and coastal shelf environments. The dominant thermal influence and reduced role of DIC on diurnal cycles of pCO_2 in the open ocean is consistent with historical observations in low productivity waters (e.g. Bates et al., 1998). Water residence times are typically lower in the open ocean compared to the coastal ocean or coral reefs (Bourgeois et al., 2016; Liu et al., 2019), and as such, the influence of localised primary production on seawater chemistry is generally

diminished. However the extent to which DIC and A_T influence the variability of open-ocean $p\text{CO}_2$ would likely have been greater had more open-ocean stations been located in subpolar latitudes (Hagens & Middelburg, 2016b; Kwiatkowski & Orr, 2018; Sarmiento & Gruber, 2006; Takahashi et al., 1993).

At a given station, extreme diurnal variability in $p\text{CO}_2$ is generally in phase with diurnal variability (Figure S4). This similarity suggests that the balance between the drivers changes little even during the extreme days. In the lower latitudes of the open ocean, extremes in variability may then be driven by conditions that act to enhance surface heat fluxes (e.g. Bates et al., 1998) or reduce the mixed layer depth. In coastal and coral reef environments, these extremes may result from conditions that are particularly favorable for primary production or physical changes that increase seawater residence times (e.g. Page et al., 2019).

Yet on some days, extreme diurnal $p\text{CO}_2$ variability is not synchronous with mean diurnal $p\text{CO}_2$ variability. This contrast is found particularly at coastal stations where there are step-changes in $p\text{CO}_2$, characteristic of upwelling events, which thus appear as a good candidate for the main driver of that asynchronous extreme diurnal variability (Figures S4-S5). Although we cannot rule out that unrealistic spikes in the data may also contribute to our analyzed extreme diurnal variability, all data are quality controlled (Sutton et al., 2019) and we find no indication of such artificial influence.

4.2 Diurnal CO$_2$ system variability within the context of climate change

Here we show that in the open ocean, extreme diurnal variability of pH can exceed 0.1, the magnitude of which is comparable to the change in the mean state of the ocean during the industrial era (Orr et al., 2005). In coastal and coral reef environments, extremes in diurnal variability are more pronounced, with daily amplitudes reaching 350 µatm for $p\text{CO}_2$ and 0.3 for pH. Diurnal variability extremes for $[\text{H}^+]$ are also 2-4 times larger in these environments.

Extremes in diurnal variability, whose amplitudes are comparable in magnitude to the change in the mean state over centuries of ocean acidification, occur across diverse marine environments. Understanding the impact of this variability on marine organisms and how it will change in response to increasing atmospheric CO_2 and climate change is needed to help assess potential changes in marine ecosystems.

Observations from natural CO_2 vents (Kerrison et al., 2011; Kwiatkowski & Orr, 2018) suggest that ocean acidification could more than double the amplitudes of diurnal variations of pCO_2 and $[H^+]$ by the end of the century. Similarly, there was nearly a three-fold amplification in the diurnal amplitudes of pCO_2 and $[H^+]$ in a mesocosm held at an average ocean fCO2 of 675 μatm relative to another held at 310 μatm (Schulz & Riebesell, 2013). Yet these vent and mesocosm studies have not been able to account for simultaneous changes in biological processes such as net primary production and calcification, which can also result in large diurnal variations in ocean CO2 variables, being driven by climate change and other anthropogenic influences. In contrast, large biological changes are already underway, such as the ongoing collapse of coral reef ecosystems (Hughes et al., 2003, 2018) and the loss of kelp forests (Krumhansl et al., 2016; Wernberg et al., 2016) and seagrasses (Waycott et al., 2009). Moreover, projections of future phytoplankton productivity are highly uncertain (Kwiatkowski et al., 2020; Taucher & Oschlies, 2011).

Current observational records remain too short to distinguish long-term trends in diurnal variability from interannual variations (see Table S3). Hence extending the current observational network is needed to assess the long-term impacts of acidification and climate change on diurnal variability of the CO_2 system. This study suggests that the impact of ocean acidification and climate change on diurnal variability of pCO_2 will differ across open ocean, coastal, and coral reef ecosystems due to the varying importance of its drivers (temperature, DIC, and A_T) , the balance among which may change in the future. Greater understanding of

the sensitivity of different marine ecosystems to present-day diurnal variability of the CO_2 system is needed to help constrain their vulnerabilities to future changes in those diurnal variations from both climate change and ocean acidification.

References

Albright, R., Takeshita, Y., Koweek, D. A., Ninokawa, A., Wolfe, K., Rivlin, T., et al. (2018). Carbon dioxide addition to coral reef waters suppresses net community calcification. *Nature*, *555*(7697), 516–519. https://doi.org/10.1038/nature25968

Bates, N. R., Takahashi, T., Chipman, D. W., & Knap, A. H. (1998). Variability of pCO2 on diel to seasonal timescales in the Sargasso Sea near Bermuda. *Journal of Geophysical Research: Solid Earth*, *103*(C8), 15567–15585. https://doi.org/10.1029/98jc00247

Bates, N. R., Astor, Y. M., Church, M. J., Currie, K., Dore, J. E., González-Dávila, M., et al. (2014). A time-series view of changing surface ocean chemistry due to ocean uptake of anthropogenic CO2 and ocean acidification. *Oceanography*, *27*(1), 126–141. https://doi.org/10.5670/oceanog.2014.16

Berg, P., Delgard, M. L., Polsenaere, P., McGlathery, K. J., Doney, S. C., & Berger, A. C. (2019). Dynamics of benthic metabolism, O2, and pCO2 in a temperate seagrass meadow. *Limnology and Oceanography*, *64*(6), 2586–2604. https://doi.org/10.1002/lno.11236

Bindoff, N. ., Cheung, J. G., Kairo, J. G., Aristegui, J., Guinder, V. A., Hallberg, R., & Al., E. (2019). Chapter 5: Changing Ocean, Marine Ecosystems, and Dependent Communities Coordinating. *IPCC Special Report on the Ocean and Cryosphere in a Changing Climate*, 447–588. https://doi.org/https://www.ipcc.ch/report/srocc/

Bourgeois, T., Orr, J. C., Resplandy, L., Terhaar, J., Ethé, C., Gehlen, M., & Bopp, L. (2016). Coastal-ocean uptake of anthropogenic carbon. *Biogeosciences*, *13*(14), 4167–4185. https://doi.org/10.5194/bg-13-4167-2016

Bresnahan, P. J., Martz, T. R., Takeshita, Y., Johnson, K. S., & LaShomb, M. (2014). Best practices for autonomous measurement of seawater pH with the Honeywell Durafet. *Methods in Oceanography*, *9*, 44–60. https://doi.org/10.1016/j.mio.2014.08.003

Burger, F. A., John, J. G., & Frölicher, T. L. (2020). Increase in ocean acidity variability and extremes under increasing atmospheric CO2. *Biogeosciences*, *17*(18), 4633–4662. https://doi.org/10.5194/bg-17-4633-2020

Caldeira, K., & Wickett, M. E. (2003). Anthropogenic carbon and ocean pH. *Nature*, *425*(6956), 365. https://doi.org/10.1038/425365a

Chan, N. C. S., & Connolly, S. R. (2013). Sensitivity of coral calcification to ocean acidification: A meta-analysis. *Global Change Biology*, *19*(1), 282–290. https://doi.org/10.1111/gcb.12011

Clark, T. D., Raby, G. D., Roche, D. G., Binning, S. A., Speers-Roesch, B., Jutfelt, F., & Sundin, J. (2020). Ocean acidification does not impair the behaviour of coral reef fishes. *Nature*, *577*(7790), 370–375. https://doi.org/10.1038/s41586-019-1903-y

Dickson, A. G., Sabine, C. L., & Christian, J. R. (2007). Guide to best practices for ocean CO2 measurements. *PICES Special Publication 3*.

Dorey, N., Lançon, P., Thorndyke, M., & Dupont, S. (2013). Assessing physiological tipping point of sea urchin larvae exposed to a broad range of pH. *Global Change Biology*, *19*(11), 3355–3367. https://doi.org/10.1111/gcb.12276

Drupp, P. S., De Carlo, E. H., Mackenzie, F. T., Sabine, C. L., Feely, R. A., & Shamberger, K. E. (2013). Comparison of CO2 dynamics and air-sea gas exchange in differing tropical reef environments. *Aquatic Geochemistry*, *19*(5–6), 371–397. https://doi.org/10.1007/s10498-013-9214-7

Feely, R. A., Sabine, C. L., Lee, K., Berelson, W., Kleypas, J., Fabry, V. J., & Millero, F. J. (2004). Impact of anthropogenic CO2 on the CaCO3 system in the oceans. *Science*, *305*(5682), 362–366. https://doi.org/10.1126/science.1097329

Frölicher, T. L., Fischer, E. M., & Gruber, N. (2018). Marine heatwaves under global warming. *Nature*, *560*(7718), 360–364. https://doi.org/10.1038/s41586-018-0383-9

Gallego, M., Timmermann, A., Friedrich, T., & Zeebe, R. E. (2018). Drivers of future

seasonal cycle changes in oceanic pCO2. *Biogeosciences*, *15*(17), 5315–5327.

https://doi.org/10.5194/bg-15-5315-2018

Garcia, H. E., Locarnini, R. A., Boyer, T. P., Antonov, J. I., Baranova, O. K., Zweng, M. M.,

et al. (2013). *World Ocean Atlas 2013, Volume 4 : Dissolved Inorganic Nutrients*

(phosphate, nitrate, silicate). NOAA Atlas NESDIS 76 (Vol. 4).

Gattuso, J.-P., & Hansson, L. (2011). Ocean acidification: background and history. *Ocean*

Acidification.

González-Dávila, M., Santana-Casiano, J. M., Petihakis, G., Ntoumas, M., Suárez de Tangil,

M., & Krasakopoulou, E. (2016). Seasonal pH variability in the Saronikos Gulf: A year-

study using a new photometric pH sensor. *Journal of Marine Systems*, *162*, 37–46.

https://doi.org/10.1016/j.jmarsys.2016.03.007

Gruber, N., Hauri, C., Lachkar, Z., Loher, D., Frölicher, T. L., & Plattner, G. K. (2012). Rapid

progression of ocean acidification in the California Current System. *Science*, *337*(6091),

220–223. https://doi.org/10.1126/science.1216773

Hagens, M., & Middelburg, J. J. (2016a). Attributing seasonal pH variability in surface ocean

waters to governing factors. *Geophysical Research Letters*, *43*(24), 12,528-12,537.

https://doi.org/10.1002/2016GL071719

Hagens, M., & Middelburg, J. J. (2016b). Generalised expressions for the response of pH to

changes in ocean chemistry. *Geochimica et Cosmochimica Acta*, *187*, 334–349.

https://doi.org/10.1016/j.gca.2016.04.012

Hauri, C., Gruber, N., Plattner, G. K., Alin, S., Feely, R. A., Hales, B., & Wheeler, P. A.

(2009). Ocean acidification in the California current system. *Oceanography*,

22(SPL.ISS. 4), 60–71. https://doi.org/10.5670/oceanog.2009.97

van Heuven, S., Pierrot, D., Rae, J. W. B., Lewis, E., & Wallace, D. W. R. (2011). MATLAB

Program Developed for CO₂ System Calculations. ORNL/CDIAC-105b. *ORNL/CDIAC-105b. Carbon Dioxide Information Analysis Center, Oak Ridge National Laboratory, U.S. Department of Energy, Oak Ridge, Tennessee*. Retrieved from http://cdiac.ornl.gov/ftp/co2sys/CO2SYS_calc_MATLAB_v1.1/

Hobday, A. J., Alexander, L. V., Perkins, S. E., Smale, D. A., Straub, S. C., Oliver, E. C. J., et al. (2016). A hierarchical approach to defining marine heatwaves. *Progress in Oceanography*, *141*, 227–238. https://doi.org/10.1016/j.pocean.2015.12.014

Hofmann, G. E., Smith, J. E., Johnson, K. S., Send, U., Levin, L. A., Micheli, F., et al. (2011). High-frequency dynamics of ocean pH: A multi-ecosystem comparison. *PLoS ONE*, *6*(12). https://doi.org/10.1371/journal.pone.0028983

Hughes, T. P., Baird, A. H., Bellwood, D. R., Card, M., Connolly, S. R., Folke, C., et al. (2003). Climate change, human impacts, and the resilience of coral reefs. *Science*. https://doi.org/10.1126/science.1085046

Hughes, Terry P., Kerry, J. T., Baird, A. H., Connolly, S. R., Dietzel, A., Eakin, C. M., et al. (2018). Global warming transforms coral reef assemblages. *Nature*, *556*(7702), 492–496. https://doi.org/10.1038/s41586-018-0041-2

Kerrison, P., Hall-Spencer, J. M., Suggett, D. J., Hepburn, L. J., & Steinke, M. (2011). Assessment of pH variability at a coastal CO2 vent for ocean acidification studies. *Estuarine, Coastal and Shelf Science*, *94*(2), 129–137. https://doi.org/10.1016/j.ecss.2011.05.025

Koweek, D. A., Dunbar, R. B., Monismith, S. G., Mucciarone, D. A., Woodson, C. B., & Samuel, L. (2015). High-resolution physical and biogeochemical variability from a shallow back reef on Ofu, American Samoa: an end-member perspective. *Coral Reefs*, *34*(3), 979–991. https://doi.org/10.1007/s00338-015-1308-9

Kroeker, K. J., Kordas, R. L., Crim, R. N., & Singh, G. G. (2010). Meta-analysis reveals

negative yet variable effects of ocean acidification on marine organisms. *Ecology Letters*. https://doi.org/10.1111/j.1461-0248.2010.01518.x

Krumhansl, K. A., Okamoto, D. K., Rassweiler, A., Novak, M., Bolton, J. J., Cavanaugh, K. C., et al. (2016). Global patterns of kelp forest change over the past half-century. *Proceedings of the National Academy of Sciences of the United States of America*, *113*(48), 13785–13790. https://doi.org/10.1073/pnas.1606102113

Kwiatkowski, L., & Orr, J. C. (2018). Diverging seasonal extremes for ocean acidification during the twenty-first century. *Nature Climate Change*, *8*(2), 141–145. https://doi.org/10.1038/s41558-017-0054-0

Kwiatkowski, L., Torres, O., Bopp, L., Aumont, O., Chamberlain, M., R. Christian, J., et al. (2020). Twenty-first century ocean warming, acidification, deoxygenation, and upper-ocean nutrient and primary production decline from CMIP6 model projections. *Biogeosciences*, *17*(13), 3439–3470. https://doi.org/10.5194/bg-17-3439-2020

Landschützer, P., Gruber, N., Bakker, D. C. E., Stemmler, I., & Six, K. D. (2018). Strengthening seasonal marine CO2 variations due to increasing atmospheric CO2. *Nature Climate Change*, *8*(2), 146–150. https://doi.org/10.1038/s41558-017-0057-x

Langenbuch, M., Bock, C., Leibfritz, D., & Pörtner, H. O. (2006). Effects of environmental hypercapnia on animal physiology: A 13C NMR study of protein synthesis rates in the marine invertebrate Sipunculus nudus. *Comparative Biochemistry and Physiology - A Molecular and Integrative Physiology*, *144*(4), 479–484. https://doi.org/10.1016/j.cbpa.2006.04.017

Lauvset, S. K., Gruber, N., Landschützer, P., Olsen, A., & Tjiputra, J. (2015). Trends and drivers in global surface ocean pH over the past 3 decades. *Biogeosciences*, *12*(5), 1285–1298. https://doi.org/10.5194/bg-12-1285-2015

Lee, K., Tong, L. T., Millero, F. J., Sabine, C. L., Dickson, A. G., Goyet, C., et al. (2006).

Global relationships of total alkalinity with salinity and temperature in surface waters of the world's oceans. *Geophysical Research Letters*, *33*(19). https://doi.org/10.1029/2006GL027207

Liu, X., Dunne, J. P., Stock, C. A., Harrison, M. J., Adcroft, A., & Resplandy, L. (2019). Simulating water residence time in the coastal ocean: a global perspective. *Geophysical Research Letters*, *46*(23), 13910–13919. https://doi.org/10.1029/2019GL085097

Mangan, S., Urbina, M. A., Findlay, H. S., Wilson, R. W., & Lewis, C. (2017). Fluctuating seawater pH/pCO2 regimes are more energetically expensive than static pH/pCO2 levels in the mussel Mytilus edulis. *Proceedings of the Royal Society B: Biological Sciences*, *284*(1865). https://doi.org/10.1098/rspb.2017.1642

Martz, T. R., Connery, J. G., & Johnson, K. S. (2010). Testing the Honeywell Durafet® for seawater pH applications. *Limnology and Oceanography: Methods*, *8*(MAY), 172–184. https://doi.org/10.4319/lom.2010.8.172

McNeil, B. I., & Matear, R. J. (2008). Southern Ocean acidification: A tipping point at 450-ppm atmospheric CO2. *Proceedings of the National Academy of Sciences of the United States of America*, *105*(48), 18860–18864. https://doi.org/10.1073/pnas.0806318105

McNeil, B. I., & Sasse, T. P. (2016). Future ocean hypercapnia driven by anthropogenic amplification of the natural CO2 cycle. *Nature*, *529*(7586), 383–386. https://doi.org/10.1038/nature16156

Meehl, G. A., & Tebaldi, C. (2004). More intense, more frequent, and longer lasting heat waves in the 21st century. *Science*, *305*(5686), 994–997. https://doi.org/10.1126/science.1098704

Munday, P. L., Dixson, D. L., Donelson, J. M., Jones, G. P., Pratchett, M. S., Devitsina, G. V., & Døving, K. B. (2009). Ocean acidification impairs olfactory discrimination and homing ability of a marine fish. *Proceedings of the National Academy of Sciences of the*

United States of America, *106*(6), 1848–1852. https://doi.org/10.1073/pnas.0809996106

Murie, K. A., & Bourdeau, P. E. (2020). Fragmented kelp forest canopies retain their ability

to alter local seawater chemistry. *Scientific Reports*. https://doi.org/10.1038/s41598-020-68841-2

O'Gorman, P. A. (2015). Precipitation Extremes Under Climate Change. *Current Climate*

Change Reports. https://doi.org/10.1007/s40641-015-0009-3

Orr, J. C., Epitalon, J. M., & Gattuso, J. P. (2015). Comparison of ten packages that compute

ocean carbonate chemistry. *Biogeosciences*, , *12*(5), 1483-1510.

https://doi.org/10.5194/bg-12-1483-2015

Orr, J. C., Fabry, V. J., Aumont, O., Bopp, L., Doney, S. C., Feely, R. A., et al. (2005).

Anthropogenic ocean acidification over the twenty-first century and its impact on

calcifying organisms. *Nature*, *437*(7059), 681–686. https://doi.org/10.1038/nature04095

Orr, J. C., Epitalon, J. M., Dickson, A. G., & Gattuso, J. P. (2018). Routine uncertainty

propagation for the marine carbon dioxide system. *Marine Chemistry*, *207*, 84–107.

https://doi.org/10.1016/j.marchem.2018.10.006

Pachauri, R. K., Allen, M. R., Barros, V. R., Broome, J., Cramer, W., Christ, R., et al. (2014).

Climate change 2014: synthesis report. Contribution of Working Groups I, II and III to

the fifth assessment report of the Intergovernmental Panel on Climate Change. Ipcc.

Page, H. N., Courtney, T. A., De Carlo, E. H., Howins, N. M., Koester, I., & Andersson, A. J.

(2019). Spatiotemporal variability in seawater carbon chemistry for a coral reef flat in

Kāneʻohe Bay, Hawaiʻi. *Limnology and Oceanography*, *64*(3), 913–934.

https://doi.org/10.1002/lno.11084

Palmer, T. N., & Räisänen, J. (2002). Quantifying the risk of extreme seasonal precipitation

events in a changing climate. *Nature*, *415*(6871), 512–514.

https://doi.org/10.1038/415512a

Pecquet, A., Dorey, N., & Chan, K. Y. K. (2017). Ocean acidification increases larval swimming speed and has limited effects on spawning and settlement of a robust fouling bryozoan, Bugula neritina. *Marine Pollution Bulletin*, *124*(2), 903–910. https://doi.org/10.1016/j.marpolbul.2017.02.057

Salisbury, J., Green, M., Hunt, C., & Campbell, J. (2008). Coastal acidification by rivers: A threat to shellfish? *Eos*, *89*(50), 513. https://doi.org/10.1029/2008EO500001

Sarmiento, J. L., & Gruber, N. (2019). *Ocean Biogeochemical Dynamics*. *Ocean Biogeochemical Dynamics*. Princeton University Press. https://doi.org/10.2307/j.ctt3fgxqx

Sasse, T. P., McNeil, B. I., Matear, R. J., & Lenton, A. (2015). Quantifying the influence of CO2 seasonality on future aragonite undersaturation onset. *Biogeosciences*, *12*(20), 6017–6031. https://doi.org/10.5194/bg-12-6017-2015

Schulz, K. G., & Riebesell, U. (2013). Diurnal changes in seawater carbonate chemistry speciation at increasing atmospheric carbon dioxide. *Marine Biology*, *160*(8), 1889–1899. https://doi.org/10.1007/s00227-012-1965-y

Seidel, M. P., DeGrandpre, M. D., & Dickson, A. G. (2008). A sensor for in situ indicator-based measurements of seawater pH. *Marine Chemistry*, *109*(1–2), 18–28. https://doi.org/10.1016/j.marchem.2007.11.013

Shadwick, E. H., Trull, T. W., Tilbrook, B., Sutton, A. J., Schulz, E., & Sabine, C. L. (2015). Seasonality of biological and physical controls on surface ocean CO2 from hourly observations at the Southern Ocean Time Series site south of Australia. *Global Biogeochemical Cycles*, *29*(2), 223–238. https://doi.org/10.1002/2014GB004906

Shamberger, K. E. F., Feely, R. A., Sabine, C. L., Atkinson, M. J., DeCarlo, E. H., Mackenzie, F. T., et al. (2011). Calcification and organic production on a Hawaiian coral reef. *Marine Chemistry*, *127*(1–4), 64–75.

https://doi.org/10.1016/j.marchem.2011.08.003

Small, D. P., Milazzo, M., Bertolini, C., Graham, H., Hauton, C., Hall-Spencer, J. M., & Rastrick, S. P. S. (2016). Temporal fluctuations in seawater pCO2 may be as important as mean differences when determining physiological sensitivity in natural systems. *ICES Journal of Marine Science*, *73*(3), 604–612. https://doi.org/10.1093/icesjms/fsv232

Sutton, A. J., Sabine, C. L., Maenner-Jones, S., Lawrence-Slavas, N., Meinig, C., Feely, R. A., et al. (2014). A high-frequency atmospheric and seawater pCO2 data set from 14 open-ocean sites using a moored autonomous system. *Earth System Science Data*, *6*(2), 353–366. https://doi.org/10.5194/essd-6-353-2014

Sutton, Adrienne J., Sabine, C. L., Feely, R. A., Cai, W. J., Cronin, M. F., McPhaden, M. J., et al. (2016). Using present-day observations to detect when anthropogenic change forces surface ocean carbonate chemistry outside preindustrial bounds. *Biogeosciences*, *13*(17), 5065–5083. https://doi.org/10.5194/bg-13-5065-2016

Sutton, Adrienne J., Feely, R. A., Maenner-Jones, S., Musielwicz, S., Osborne, J., Dietrich, C., et al. (2019). Autonomous seawater pCO 2 and pH time series from 40 surface buoys and the emergence of anthropogenic trends. *Earth System Science Data*, *11*(1), 421–439. https://doi.org/10.5194/essd-11-421-2019

Takahashi, T., Olafsson, J., Goddard, J. G., Chipman, D. W., & Sutherland, S. C. (1993). Seasonal variation of CO2 and nutrients in the high-latitude surface oceans: A comparative study. *Global Biogeochemical Cycles*, *7*(4), 843–878. https://doi.org/10.1029/93GB02263

Takahashi, T., Sutherland, S. C., Chipman, D. W., Goddard, J. G., & Ho, C. (2014). Climatological distributions of pH, pCO2, total CO2, alkalinity, and CaCO3 saturation in the global surface ocean, and temporal changes at selected locations. *Marine Chemistry*, *164*, 95–125. https://doi.org/10.1016/j.marchem.2014.06.004

Taucher, J., & Oschlies, A. (2011). Can we predict the direction of marine primary production change under global warming? *Geophysical Research Letters*, *38*(2). https://doi.org/10.1029/2010GL045934

Thomsen, J., Gutowska, M. A., Saphörster, J., Heinemann, A., Trübenbach, K., Fietzke, J., et al. (2010). Calcifying invertebrates succeed in a naturally CO2-rich coastal habitat but are threatened by high levels of future acidification. *Biogeosciences*, *7*(11), 3879–3891. https://doi.org/10.5194/bg-7-3879-2010

Vinet, L., & Zhedanov, A. (2011). A "missing" family of classical orthogonal polynomials. *Journal of Physics A: Mathematical and Theoretical*, *44*(8). https://doi.org/10.1088/1751-8113/44/8/085201

Watson, S. A., Fields, J. B., & Munday, P. L. (2017). Ocean acidification alters predator behaviour and reduces predation rate. *Biology Letters*, *13*(2). https://doi.org/10.1098/rsbl.2016.0797

Waycott, M., Duarte, C. M., Carruthers, T. J. B., Orth, R. J., Dennison, W. C., Olyarnik, S., et al. (2009). Accelerating loss of seagrasses across the globe threatens coastal ecosystems. *Proceedings of the National Academy of Sciences of the United States of America*, *106*(30), 12377–12381. https://doi.org/10.1073/pnas.0905620106

Weiss, R. F. (1974). Carbon dioxide in water and seawater: the solubility of a non-ideal gas. *Marine Chemistry*, *2*(3), 203–215. https://doi.org/10.1016/0304-4203(74)90015-2

Wernberg, T., Bennett, S., Babcock, R. C., De Bettignies, T., Cure, K., Depczynski, M., et al. (2016). Climate-driven regime shift of a temperate marine ecosystem. *Science*, *353*(6295), 169–172. https://doi.org/10.1126/science.aad8745

Xue, L., Cai, W. J., Hu, X., Sabine, C., Jones, S., Sutton, A. J., et al. (2016). Sea surface carbon dioxide at the Georgia time series site (2006-2007): Air-sea flux and controlling processes. *Progress in Oceanography*, *140*, 14–26.

https://doi.org/10.1016/j.pocean.2015.09.008

Yan, H. Q., Yu, K. F., Shi, Q., Tan, Y. H., Zhang, H. L., Zhao, M. X., et al. (2011). Coral reef
ecosystems in the South China Sea as a source of atmospheric CO2 in summer. *Chinese
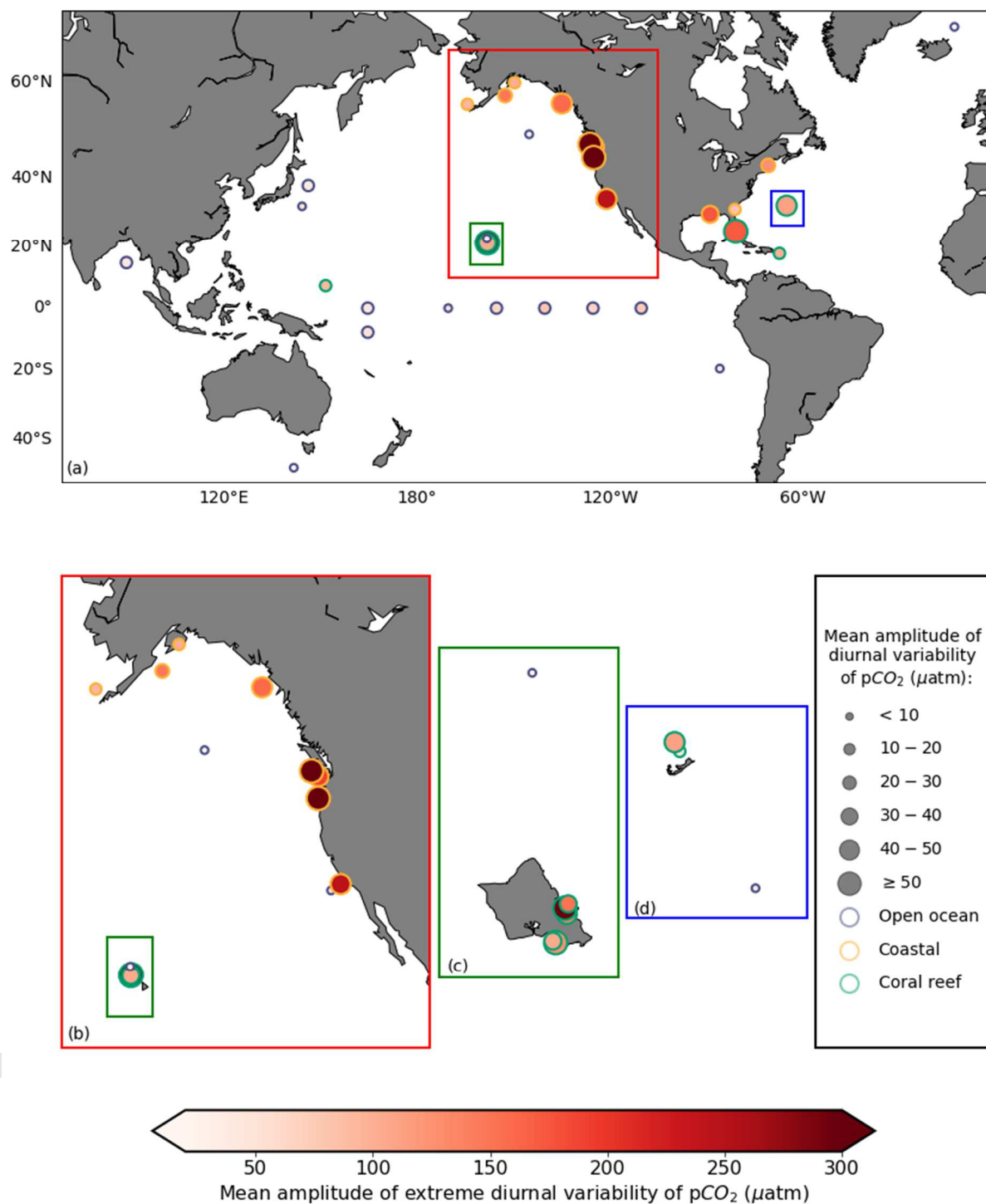Science Bulletin*, *56*(7), 676–684. https://doi.org/10.1007/s11434-011-4372-8

Figure 1. The peak-to-peak amplitudes of mean and extreme diurnal pCO_2 variability (µatm) (a) globally, (b) in the eastern Pacific, (c) in Hawaii, and (d) in Bermuda. Circle size indicates the mean amplitude of the diurnal variability of pCO_2 at a given station, while the interior color indicates the mean amplitude of extreme diurnal variability (99th percentile days). The exterior line color of circles indicate the station type (open ocean, coastal, or coral reef).
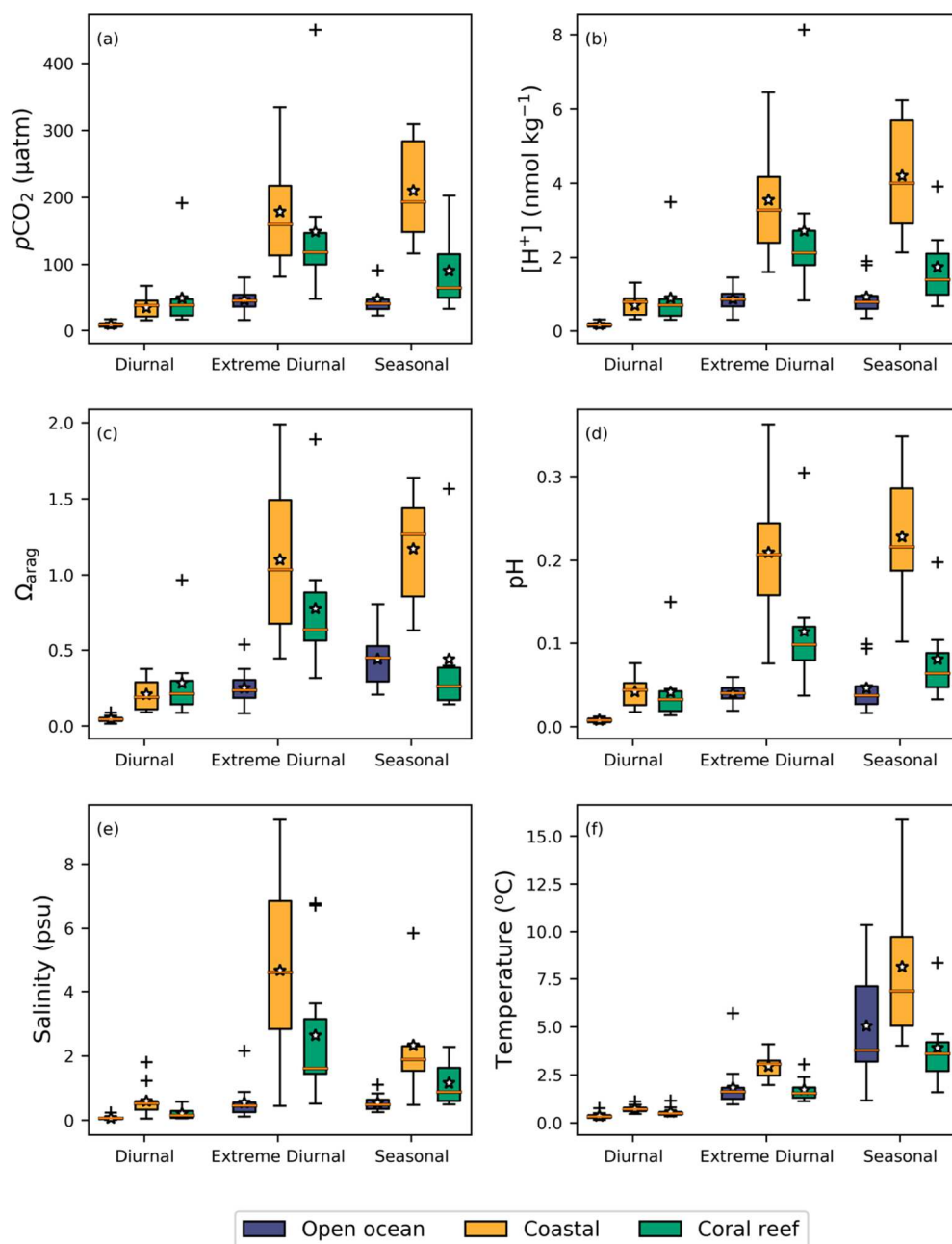
Figure 2. Diurnal, extreme diurnal, and seasonal cycle amplitudes of (a) pCO_2 (µatm), (b) [H$^+$] (total scale, nmol kg^{-1}), (c) Ω_{arag}, (d) pH on the total scale, (e) salinity on the practical salinity scale, and (f) temperature (°C). Each boxplot shows the mean diurnal, extreme diurnal, and seasonal amplitudes of stations of a given type. For diurnal cycles, in the open ocean n=16, for coastal stations n=11, and for coral reef stations n=10. For seasonal cycles, in the open ocean n=9, for coastal stations n=6, and for coral reef stations n=9. Boxplots show the multi-station mean (stars), the median (red lines), the interquartile range IQR (boxes), the values furthest from upper and lower quartiles but within 1.5*IQR (whiskers), and the outliers (pluses).
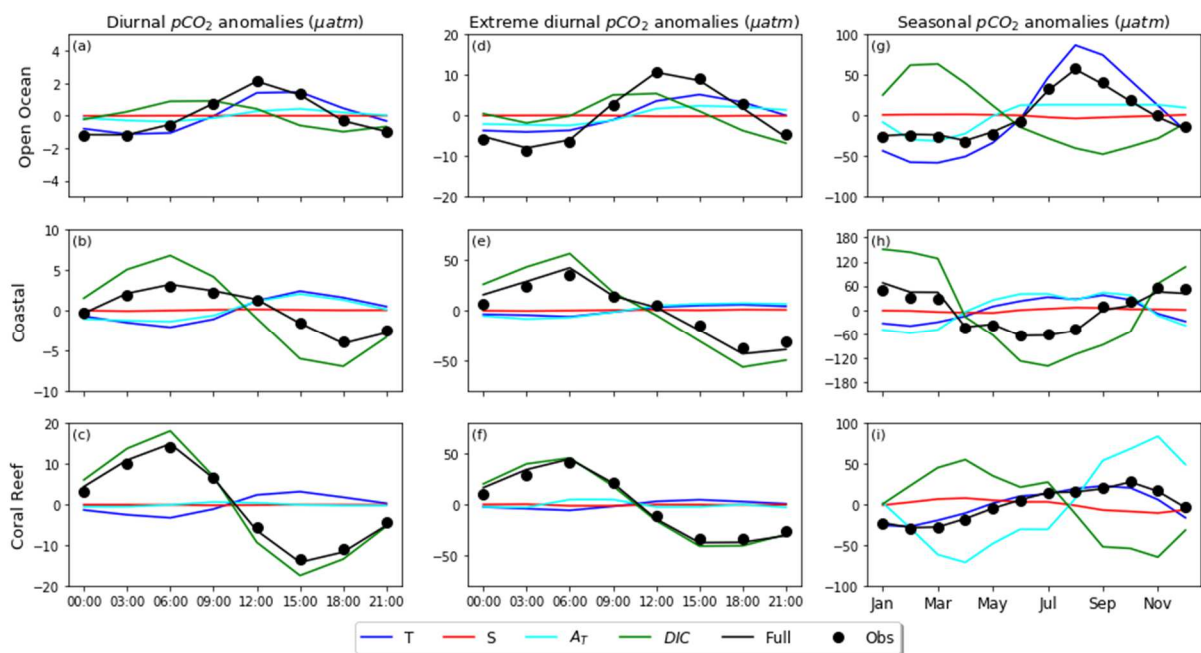
Figure 3. Deconvolution of the drivers of diurnal, extreme diurnal, and seasonal pCO_2 variability based on Equation 2. Shown across station types are the observed diurnal, extreme diurnal, and seasonal pCO_2 anomalies (black dots) and the sum of the full decomposition (black lines) as well as the contributions attributable to variations in temperature (blue), salinity (red), DIC (green) and A_T (cyan). For diurnal and extreme diurnal variability, the observed anomalies and deconvolved contributions are averaged across all stations of the same type (open ocean, coastal, and coral reef). Seasonal variability is shown for one station of each station type (KEO station for open ocean, Cape Elizabeth station for coastal ocean, and La Parguera station for coral reef), while remaining stations are provided in the supplementary material (Figures S1-S3).

Diurnal pCO_2 anomalies (μatm) — Extreme diurnal pCO_2 anomalies (μatm) — Seasonal pCO_2 anomalies (μatm)

T — S — A_T — DIC — Full — Obs